The Riddle of Resorcinol Crystal Growth Revisited: Molecular Dynamics Simulations of α-Resorcinol Crystal−Water Interface

Mumtaz Hussain and Jamshed Anwar*

Contribution from the Computational Pharmaceutical Sciences Laboratory, Department of Pharmacy, King's College London, Franklin-Wilkins Building, 150 Stamford Street, London SE1 8WA, United Kingdom

Abstract: The mechanism by which solvent exerts its effect during the process of crystallization is poorly understood. An important and ongoing problem is the uneven growth of the faces {011} and {01$\bar{1}$} of α-resorcinol in water. Growth occurs mainly at the {0$\bar{1}\bar{1}$} surface. In an attempt to determine the mechanism, molecular-dynamics simulations have been carried out of the two surfaces in contact with water. The dynamical properties of the water close to the surface as well as the overall interaction energies of the water with the respective faces have been calculated. The strongest water-binding sites have also been determined and energetically characterized. The data indicate that the adsorption of water molecules is stronger at the slower growing {011} face, with the strongest binding occurring at specific sites on this face. The motion of the water molecules in the surface layer at this face is also more localized and restricted compared with that at the faster growing {0$\bar{1}\bar{1}$} face. The binding sites at the {011} surface are not within the grooves that are present at this surface but are located above the outermost part of the crystal surface. The water molecules form strong hydrogen bonds with the limited number of hydroxyl oxygens of the resorcinol molecules protruding from the surface. The overall inference is that the stronger binding of the water molecules at the {011} surface serves to retard crystal growth, rather than enhancing it as predicted by the surface roughening theory.

Introduction

The choice of solvent during crystallization can influence both the structure and habit of the resulting crystals. However, the mechanism of action by which solvent exerts its influence is still a matter of debate. There are two distinct hypotheses that attempt to explain the effect of solvent on crystal growth. In the surface roughening hypothesis[1] the interaction of the solvent with specific crystal faces is considered to reduce the surface tension. The consequence is a transition from a smooth to a rough interface and a resultant increase in the rate of growth of the affected faces. On the molecular level, the solvent reduces the edge energy, thus lowering the barrier for the two-dimensional nucleation required for initiating the growth of the next layer. The alternative hypothesis proposes that any preferential adsorption of the solvent to a given crystal face will inhibit the growth of that particular face,[2] since the solute would be in competition with the solvent molecules for the growth sites. Attachment of solute would require removal of the bound solvent, which would be an additional energy barrier. This latter theory of adsorption resulting in inhibition is consistent with the mechanism of action of tailor-made additives

on crystal growth.[3] Selective adsorption of tailor-made additives onto a given face results in inhibition of growth of that face.

An effective way of investigating the effects of solvent on crystal growth is to focus on polar crystals.[4] Unequal growth of polar crystals along the polar axis tends to be dominated by crystal−solvent interactions. The few studies that have attempted to examine the effect of solvent indicate that neither of the two hypotheses, surface roughening or adsorption−inhibition, needs be the definitive mechanism. For some systems, e.g., *N-n*-octyl-D-gluconamides crystallizing from water, the differences in the crystal growth of specific faces are related to the hydrophilicity of the face[5] and inversely to the average binding energy of solvent to the face.[6] These observations thus support the adsorption−inhibition hypothesis. However, with other systems, e.g., (*R,S*)-alanine and γ-glycine, the experimental observations of faster growth along one side of the polar axis can only be explained by a complex, relay-type mechanism that does not fall in either camp.[7]

The difficulty in elucidating the mechanism of action of solvent results from the fact that the molecular structure and dynamics of the crystal−solvent interface are not entirely accessible by direct experiment. In favorable systems, the space- and time-averaged structural aspects of the crystal−solvent interface can be characterized by grazing-incidence X-ray diffraction.[8] A complementary approach is to utilize potential

* To whom correspondence should be addressed. E-mail: jamshed.anwar@kcl.ac.uk.

(1) (a) Bourne, J. R.; Davey, R. J. *J. Cryst. Growth* **1976**, *36*, 278−287. (b) Bourne, J. R.; Davey, R. J. *J. Cryst. Growth* **1976**, *36*, 287−296. (c) Bennema, P.; van Eerden, J. P. In *Morphology of Crystals*; Terra Scientific Publishing Co.: Tokyo, 1977; pp 1−75. (d) Shimon, L. J. W.; Vaida, M.; Addadi, L.; Lahav, M.; Leiserowitz, L. *J. Am. Chem. Soc* **1990**, *112*, 6215. (e) Bennema, P.; Gilmer, G. In *Crystal Growth: An Introduction*; Hartman, P., Ed.; North-Holland, Amsterdam, 1973; p 274.

(2) (a) Weissbuch, I.; Popovitibiro, R.; Lahav, M., Leiserowitz, L. *Acta Crystallogra., Sect. B* **1995**, *51*, 115. (b) Wells, A. F. *Discuss. Faraday Soc.* **1949**, *5*, 197. (c) Berkovitch-Yellin, Z. *J. Am. Chem. Soc.* **1985**, *107*, 8239. (d) Davey, R. J.; Milisavljevic, B.; Bourne, J. R. *J. Phys. Chem.* **1988**, *92*, 2032−2036.
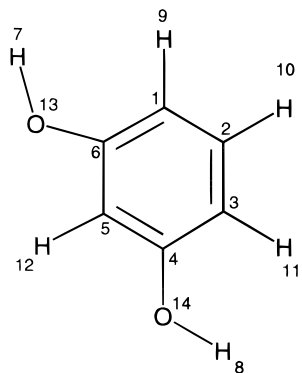
(3) Weissbuch, I.; Shimon, L. J. W.; Landau, K. M.; Popovitz-Biro, R.; Berkovitch-Yellin, Z.; Addadi, L.; Lahav, M.; Leiserowitz, L. *Pure Appl. Chem.* **1986**, *58* (6), 947−954. (b) Weissbuch, I.; Popovitz-Biro, R.; Lahav, M.; Leiserowitz, L. *Acta Crystallogr.* **1995**, *B51*, 115.

(4) Curtin, D. Y.; Paul, I. C. *Chem. Rev.* **1981**, *81* (6), 525−540.

(5) Wang, J.; Leiserowitz, L.; Lahav, M. *J. Phys. Chem.* **1992**, *96*, 15−16.

(6) Khoshkoo, S.; Anwar, J. *J. Chem. Soc., Faraday Trans.* **1996**, *92* (6), 1023−1025.

(7) Weissbuch, I.; Addadi, L.; Lahav, M.; Leiserowitz, L. *Science* **1991**, *253*, 637−645.

8584   *J. Am. Chem. Soc., Vol. 121, No. 37, 1999*

Hussain and Anwar

Figure 1. Molecular structure of resorcinol.

Figure 2. Simulation cell comprising a crystal lamina of α-resorcinol with the faces $\{0\bar{1}\bar{1}\}$ and $\{011\}$ exposed to water. Periodic boundaries exist in all three directions.

energy calculations and computer simulations based on the atom−atom potential method.[9] While it is possible to simulate crystallization from melt for realistic systems,[10] explicit simulation of crystallization from a solvent still represents a challenge. The basic problem is that the latter process is characterized by long time scales. Success has been achieved using simple models comprising individual solute and solvent atoms characterized by a Lennard-Jones potential,[11] and these studies are considerably enhancing our understanding. Real molecular systems, however, remain inaccessible. In view of this, simulations are restricted to examining the interaction and behavior of solvent at the surface of a *predefined* crystal. Notable investigations of this type include the crystal−water interface of ice,[12] sodium chloride,[13] urea,[14] resorcinol,[6] and *N-n*-octyl-D-gluconamides.[6]

The riddle of α-resorcinol (Figure 1) concerning the uneven growth of the faces $\{011\}$ and $\{0\bar{1}\bar{1}\}$ along the polar axis in an aqueous solution is an important and outstanding problem.[15,16] Growth occurs primarily along the $\{0\bar{1}\bar{1}\}$ face.[17] Due to the polar axis, both faces are expected to grow evenly provided the solvent−surface interaction at the two faces is about the same. Structurally, the $\{0\bar{1}\bar{1}\}$ face is relatively flat, exposing primarily hydroxyl oxygen atoms of the resorcinol molecules but not their hydrogen substituents. Three out of four of the hydroxyl hydrogens are involved in hydrogen bonds linking the resorcinol molecules within the layer. The fourth hydroxyl is buried within the layer and emerges at the $\{011\}$ face. The $\{011\}$ face consists of grooves between protruding molecules and exposes mostly aromatic hydrogens and a limited number (one out of a possible four) of hydroxyl hydrogens. Since aromatic hydrogens of phenol-like molecules are known to form C−H$\cdots$O hydrogen bonds,[18] the $\{0\bar{1}\bar{1}\}$ and $\{011\}$ faces have been referred to as basic and acidic, respectively.[16]

The question of how the aqueous solvent exerts its influence across the resorcinol polar axis has been investigated using static

potential energy calculations of the interaction of water with the crystal surface[16] and Monte Carlo simulations of the crystal−water interface.[6] The findings from these studies, however, were inconclusive. These studies suggest that the lower rate of growth of the $\{011\}$ face may be due to strong and specific interactions of water within the grooves present at this face. What is missing is a dynamic picture of the solvent behavior at the crystal−solvent interface. One needs to identify any important sites on the crystal surface, the energies of interaction of the solvent molecules at these sites, and residency times or diffusion rate constants of the solvent molecules. These considerations suggest a molecular dynamics simulation of the $\{011\}$ and $\{0\bar{1}\bar{1}\}$ crystal−water interfaces as the next logical step.

This paper presents a molecular dynamics (MD) simulation study of the $\{011\}$ and $\{0\bar{1}\bar{1}\}$ interfaces of crystalline α-resorcinol with water. The data yield a detailed picture of both the dynamics and energetics of water interactions at the two surfaces, which has been found invaluable toward elucidating the mechanism of action of the solvent.

Molecular Dynamics Simulations

The MD simulations were performed using the DL_POLY package.[19] The simulation cell consisted of a thin block of α-resorcinol crystal exposing the $\{0\bar{1}\bar{1}\}$ and $\{011\}$ faces to water (Figure 2). Periodic boundary conditions were applied in all three dimensions. Thus, the resorcinol crystal was infinite in the *y* and *z* directions but limited in the *x* dimension. When simulating interfaces using such boundary conditions, it is important to ensure that the solvent molecules in the simulation system do not simultaneously see both faces of the crystal. This constraint prevents one crystal face from influencing the water structure at the other face. Therefore, the thickness of the water layer separating the two faces must be at least 4 times the cutoff radius. Likewise, the thickness of the crystal slab must be greater than 2 times the cutoff. This prevents water molecules that are in juxtaposition to one of the crystal faces from seeing (across the crystal boundary) water molecules at the other face. The cutoff was 1.1 nm. The thickness of the crystal slab was 6.0 nm, while that of the water layer was typically about 7.0 nm, both well within the constraints. A typical system consisted of 432 molecules of resorcinol and 2117 molecules of water.

The SPC model[20] for water was used at a starting system water density of approximately 1.0 g/cm^3. The resorcinol molecule was described by a force field form comprising intramolecular terms (bonds, angles, and dihedrals), a Lennard-Jones term for the nonbonded dispersion interactions, and a Coulombic interaction term. Partial

(8) Edgar, R.; Schultz, T. M.; Rasmussen, F. B.; Feidenhans'l, R.; Leiserowitz, L. *J. Am. Chem. Soc.* **1999**, *121*, 632−637.

(9) Pertsin, A. J.; Kitaigorodski, A. I. In *The Atom-Atom Potential Method*; Springer Series in Chemical Physics; Springer-Verlag: Berlin, 1987; Vol. 43.

(10) Esselink, K.; Hilbers, P. A. J.; van Beest, B. W. H. *J. Chem. Phys.* **1994**, *101* (10), 9033−9041.

(11) Anwar, J.; Boateng, P. K. *J. Am. Chem. Soc.* **1998**, *120*, 9600−9604.

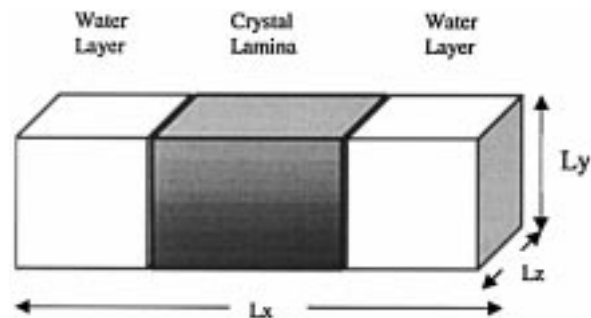(12) Karim, O. A.; Haymet, A. D. J. *J. Chem. Phys.* **1988**, *89* (11), 6889−6896.

(13) Shinto, H.; Sakakibara, T.; Higashitani, K. *J. Phys. Chem.* **1998**, *102*, 1974−1981.

(14) Boek, E. S.; Briels, W. J.; van Eerden, J.; Field, D. *J. Chem. Phys.* **1992**, *96* (9), 7010−7018.

(15) Wells, A. F. *Discuss. Faraday Soc.* **1949**, *5*, 197.

(16) Wireko, F. C.; Shimon, L. J. W.; Frolow, F.; Berkovitch-Yellin, Z.; Lahav, M.; Leiserowitz, L. *J. Phys. Chem.* **1987**, *91*, 472−481.

(17) Shimon, L. J. W.; Wireko, F. C.; Wolf, J.; Weissbuch, L.; Addadi, L.; Berkovitch-Yellin, Z.; Lahav, M.; Leiserowitz, L. *Mol. Cryst. Liq. Cryst.* **1986**, *137*, 67.

(18) Berkovitch-Yellin, Z.; Leiserowitz, L. *Acta Crystallogr*. **1984**, *B40*, 159.

(19) DL_POLY is a package of molecular simulation routines: Smith, W.; Forester, T. R. *DL_POLY*; The Council for the Central Laboratory of the Research Councils: Daresbury Laboratory, Daresbury, Warrington, U.K., 1996.

(20) Berendsen, H. J. C.; Postma, J. P. M.; van Gunsteren, W. F.; Hermans, J. In *Intermolecular Forces*; Pullman, B., Ed.; Reidel: Dordrecht, Holland, 1981; p 331.

Table 1. Partial Charges for the α-Resorcinol Molecule Determined Using Electrostatic Potential Fitting to the SCF Wavefunction (6-31G**) of the Optimized Molecule

atom index	atom	electronic charge/electrons
1	C1	−0.569
2	C2	0.108
3	C3	−0.569
4	C4	0.611
5	C5	−0.575
6	C6	0.611
7	H1	0.456
8	H2	0.456
9	H3	0.198
10	H4	0.133
11	H5	0.198
12	H6	0.266
13	O1	−0.622
14	O2	−0.622

Table 2. Crystal Force Field Evaluation[a]

force field	exptl	AMBER	% dev	OPLS	% dev	CHARMM	% dev
A/Å	10.530	10.74	1.99	10.76	2.18	11.02	4.65
B/Å	9.530	10.34	8.50	10.38	8.92	10.56	10.81
C/Å	5.660	5.34	5.65	5.26	7.07	5.45	3.71
α/deg	90.0	90.01	0.01	89.91	0.10	90.02	0.02
β/deg	90.0	90.01	0.01	89.98	0.02	90.10	0.11
γ/deg	90.0	89.96	0.04	89.89	0.12	89.89	0.12
lattice energy/ kcal mol^{-1}	22.1	24.7		25.9		24.9	

[a] Deviation of unit cell parameters from experiment[30] for the α-resorcinol crystal after a 5 ps molecular dynamics (constant stress) simulation at 298 K as a function of force field. Corresponding lattice energies are also compared with the experimental sublimation enthalpy.[26]

charges for resorcinol were determined from electrostatic potential fitting to the SCF wave function (6-31G**) of the optimized molecule. The charges are given in Table 1.

Parameters from the force fields CHARMM,[21] OPLS,[22] and AMBER[23] were evaluated for resorcinol by performing a 5 ps simulation of the α-resorcinol crystal (3 × 3 × 5 unit cells) in the Parrinello-Rahman (constant stress) NPT ensemble[24] at a temperature of 298 K to assess the stability of the crystal lattice. The long-range coulomb interactions were calculated using Ewald summation.[25] Real-space cutoff was 1.1 nm. The resulting lattice parameters and the corresponding lattice energies from the simulations as a function of force field are tabulated in Table 2. Of the three force fields, the AMBER parameters gave the lowest deviation in the lattice parameters and the closest lattice energy value (24.7 kcal/mol) to the known experimental sublimation enthalpy[26] (22.1 kcal/mol). The low lattice parameter deviations and the respectable parity between the lattice energy and the sublimation enthalpy indicate that the AMBER parameters are reasonably accurate in describing the α-resorcinol crystal. The AMBER force field was therefore chosen and employed for the resorcinol crystal−water interface simulations.

Two simulations of the resorcinol−water interface were carried out. In the first simulation the Coulombic interactions were calculated using Ewald summation, while for the second the Coulombic interactions were restricted to the cutoff employed for the dispersion term. The

(21) Smith, J. C.; Karplus, M. *J. Am. Chem. Soc* **1992**, *114*, 803−812.
(22) Jorgensen, W. L.; Maxwell, D. S.; Tirado-Rives, J. *J. Am. Chem. Soc*. **1996**, *117*, 11225−11236.
(23) Cornell, W. D.; Cieplak, P.; Bayly, C. I.; Gould, I. R.; Merz, K. M., Jr.; Ferguson, D. M.; Spellmeyer, D. C.; Fox, T.; Caldwell J. W.; Kollman, P. A. *J. Am. Chem. Soc*. **1995**, *117*, 5179−5197.
(24) (a) Parinnello, M.; Rahman, A. *Phys. Rev. Lett*. **1980**, *45*, 1196. (b) Parinnello, M.; Rahman, A. *J. Appl. Phys*. **1980**, *52*, 7182.
(25) Ewald, P. *Ann. Phys*. **1921**, *64*, 253.
(26) Bender, R.; Bieling, V.; Mauer, G. *J. Chem. Thermodyn*. **1983**, *15*, 585−594.
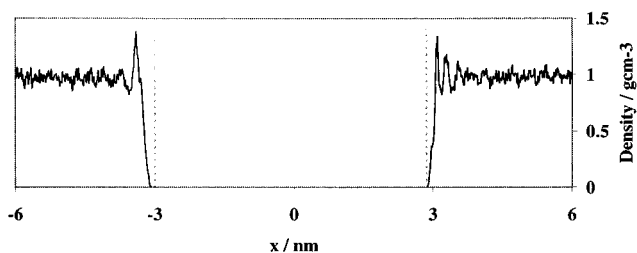
Figure 3. Water density profile across the simulation cell averaged over 100 ps for the Ewald summation simulation. The crystal boundary, defined by the center-of-mass positions of the surface resorcinol molecules, is shown by the vertical dotted line. The slower growing {011} face is on the right.

Table 3. Water Layer Properties

surface	layer	range (distance from center of simulation cell)/nm	number of water molecules	density/ g cm^{-3}
{011}	layer 1	2.86−3.20	109	1.09
	layer 2	3.20−3.38	69	0.95
	bulk	5.00−6.00	284	0.94
{0$\bar{1}\bar{1}$}	layer 1	3.05−3.35	163	1.13
	bulk	5.00−6.00	283	0.94

reason for carrying out these two simulations was to ascertain as to what extent the results are influenced by the choice of treatment of the Coulombic terms. For simulations of water between metal surfaces, the use of Ewald summation is known to significantly improve the match between the observed and the calculated structural ordering of the water.[27]

The simulations were carried out in a constant NPT ensemble at a temperature of 298 K and 1 atm pressure. The time step was 2 fs. The cutoff was 1.1 nm for the dispersion interactions. The crystal was kept static, and only the water molecules were allowed freedom during the simulation. There was uncertainty as to whether the crystal structure would remain stable in the presence of water. In setting up the simulation box, the crystal structure was minimized prior to immersion in the water and then again in the presence of water.

Each crystal−water interface simulation was carried out initially for 100 ps to allow equilibration. This was followed by a production run of 100 ps. System trajectories were sampled every 50 time steps, being equivalent to 0.10 ps.

Results and Analysis

The results presented, unless stated otherwise, refer to the simulation employing Ewald summation.

Density Profiles. The system was divided into segments of 0.015 nm along the *x*-axis. The center-of-mass density of water was then calculated in each segment. The resulting water density profile is shown in Figure 3. The profile reveals a single strong peak at the {0$\bar{1}\bar{1}$} face and at least two well-defined sharp peaks at the {011} face. The peaks represent distinct surface layers of water in which the molecules are more localized compared to the surrounding bulk water. The widths of the peaks have been used to define the layers of water at the surface. The layer definitions and properties are tabulated in Table 3. Moving away from the surfaces, the density begins to become more uniform, indicating that the ordering of the water molecules is restricted to the surfaces. The features of the water density profile obtained for the non-Ewald simulation (not shown) are identical to the profile obtained from the simulation employing Ewald summation.

Trajectory Projections. It is useful to examine the extent of the motion of the water molecules at varying distances from

(27) Shelley, J. C.; Berard, D. R. In *Reviews in Computational Chemistry*; Lipkowitz, K. B., Boyd, D. B., Eds.; John Wiley & Sons: New York, 1998; Vol. 12, pp 137−275.

Table 4. Diffusion Rate Constants for Water in the Surface Layers of Water and in a Segment of Water at 5.0−6.0 nm from the Center of the Simulation Cell
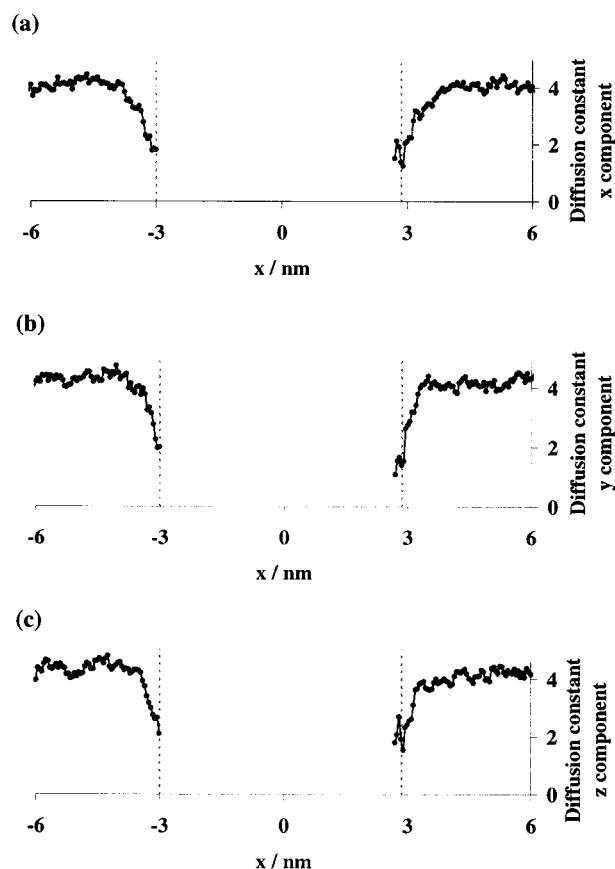
surface	layer	$D/10^{-9}\,m^2\,s^{-1}$	$D_x/10^{-9}\,m^2\,s^{-1}$	$D_y/10^{-9}\,m^2\,s^{-1}$	$D_z/10^{-9}\,m^2\,s^{-1}$
{011}	layer 1	2.11 (0.14)[a]	1.80 (0.05)	2.36 (0.20)	2.27 (0.19)
	layer 2	3.42 (0.13)	2.94 (0.07)	3.66 (0.10)	3.58 (0.07)
	bulk	4.34 (0.11)	4.29 (0.14)	4.23 (0.37)	4.45 (0.26)
{0$\bar{1}\bar{1}$}	layer 1	3.04 (0.13)	2.82 (0.28)	3.20 (0.03)	3.36 (0.27)
	bulk	4.24 (0.14)	4.40 (0.11)	4.27 (0.17)	4.26 (0.12)

[a] The estimated standard deviations are given in parentheses.
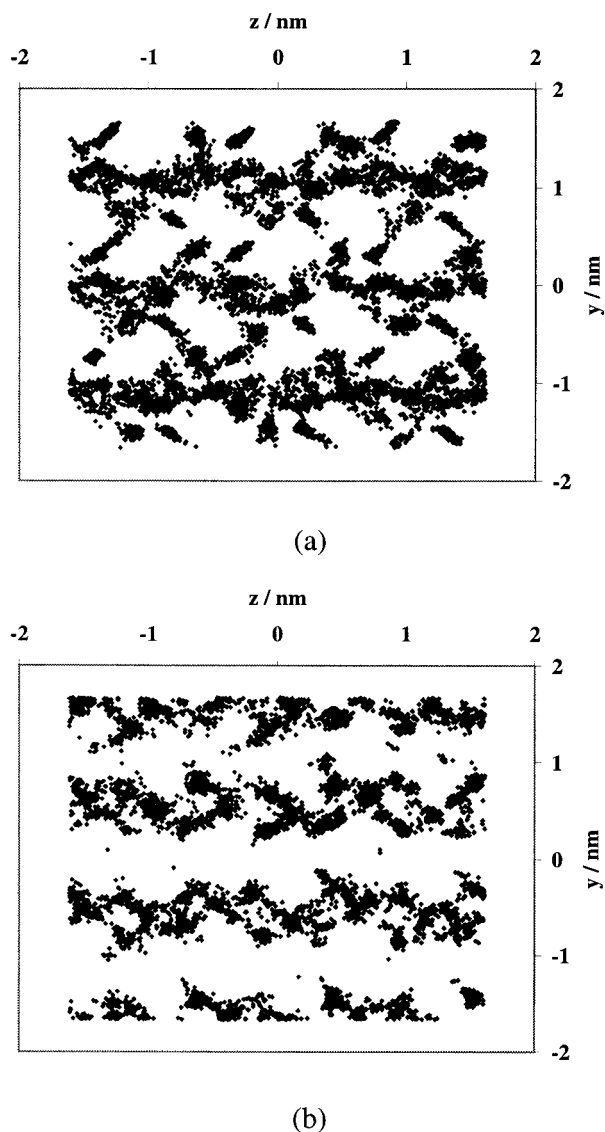
Figure 4. Center-of-mass trajectory projections for the water molecules in the first surface layer plotted in the plane of the crystal surface over a 100 ps period for the (a) {011} and (b) {0$\bar{1}\bar{1}$} crystal−water interface.

Figure 5. Diffusion rate constant of water (10^{-9} m^2 s^{-1}) in 0.05 nm segments along the *x* dimension of the simulation cell in the (a) *x*, (b) *y*, and (c) *z* dimension calculated over a 100 ps trajectory. The crystal boundary, defined by the center-of-mass positions of the surface resorcinol molecules, is shown by the vertical dotted line. The slowest growing {011} face is on the right. Data appearing within the crystal at the {011} surface are for molecules that are present within the grooves at this surface.

the crystal surface. This can be done pictorially by plotting the center-of-mass trajectories of water molecules in a defined layer in the plane of the crystal surface (y−z plane). The resulting trajectory projections for the first surface layer (as defined from the water density profile) for the two crystal faces are shown in Figure 4. The trajectory projections for both faces show localization of the water to corrugated and restrictive channels running along the *z*-axis of the system. The first layer of water at the {011} face also reveals additional islands located between the channels where the water molecules are highly localized during the simulation. Trajectory projections (not shown) of segments of water moving away from the crystal show the water

motion becoming more diffuse. In the furthest segment from the crystal surface the trajectory projections become altogether uniform.

Diffusion. The diffusion of the water molecules was characterized in the surface layers (as defined from the water density profile) and the bulk and also in 0.05 nm segments along the *x*-axis of the system. The effective diffusion constants for the surface layers and for a segment of bulk water are presented in Table 4. The diffusion constants in the *x*, *y*, and *z* dimension of the simulation cell for the 0.05 nm segments are plotted as a function of distance along the *x*-axis in Figure 5. The diffusion constants were calculated as detailed by Boek et al.[14] The calculation for each segment/layer was over periods of 10 ps and then averaged over the entire production run.

The diffusion constants for water in the segments closest to the surface of the slower growing {011} face are consistently lower than the respective values for the {0$\bar{1}\bar{1}$} face. This

Table 5. Crystal−Water Interaction Energies for the {011} and the {0$\bar{1}\bar{1}$} Surfaces of α-Resorcinol against Water

surface	Coulombic/ mJ m^{-2}	Lennard-Jones/ mJ m^{-2}	total/ mJ m^{-2}
{011}	−132.07	−12.58	−144.65
{0$\bar{1}\bar{1}$}	−110.69	−15.28	−125.97

indicates that the water at the surface of the slower growing {011} face remains much more localized in position. In general, the diffusion constants are lower for the water molecules closest to the surfaces, i.e., those within the channels or grooves present at the surfaces, and gradually increase as one moves away from the surfaces. For the slow growing {011} face, all three anisotropic diffusion constants show a small peak with an associated minimum close to the surface. The diffusion constant is lowest for the innermost molecules and, on moving away, shows an increase followed by a decrease leading to a minimum and then begins to increase again. The implication is that, other than the innermost water molecules, there is an additional layer whose motion is strongly restricted. This layer corresponds to the strongest-bound water molecules at this surface (see below). Comparison of the anisotropic diffusion coefficients (Table 4) shows that the diffusion of the water in the surface layers is slower in the *x* direction compared with the *y* and *z* directions. This is expected, since the transfer of the water molecules from one surface layer to the next (or to the bulk water) is likely to be restricted. On moving away from the crystal surface, the coefficients become larger and plateau as the water begins to behave much like bulk water. The coefficient obtained for the water furthest from the crystal surfaces compares well with previous calculated values for SPC bulk water.[28] This confirms that the dimensions of the simulation cell were adequate, particularly the thickness of the water between the two crystal faces.

Crystal−Water Interaction Energy. Molecular dynamics packages that are currently available do not give a breakdown of the potential energy for either the individual molecular species or the interspecies interaction.

Therefore, the crystal−water interaction energies and the individual water molecule binding energies were calculated from the trajectories. The crystal−water interaction energies for both surfaces {011} and {0$\bar{1}\bar{1}$} are given in Table 5. These energies reveal a higher affinity of water for the slower growing {011} face, the actual energy being about 16% lower (higher in magnitude but negative) than that for the {0$\bar{1}\bar{1}$} face. Breakdown of the energies shows that the Coulombic component is largely responsible.

The crystal−water interaction energy with a change in sign is commonly referred to as the work of adhesion W_a. It is related to the solid/liquid interfacial free energy, γ_{LS}, by the Dupre equation

$$W_a = \gamma_L + \gamma_S - \gamma_{LS}$$

where γ_L and γ_S are the surface free energies of the liquid and solid phase, respectively.

The surface free energy of a solid, γ_S, can be estimated from the interaction energy (work of cohesion W_c) between two halves of a crystal bisected perpendicular to the required axis. The appropriate equation is $W_c = 2\gamma_S$. The determined γ_S is at 0 K and does not take into account surface reconstruction. Substituting W_a for a given face of resorcinol (125.97 mJ m^{-2} for {0$\bar{1}\bar{1}$}

(28) van der Spoel, D.; van Maaren, P. J.; Berendsen, H. J. C. *J. Chem. Phys.* **1998**, *108*, 24.

Table 6. Binding Energies and Diffusion Constants of the 14 Strongest-Bound Water Molecules at the {011} Surface

| binding energy/ kJ mol^{-1}	diffusion constant/ 10^{-9} m^2 s^{-1}
−36.51	0.23
−36.83	0.10
−33.88	0.19
−35.95	0.19
−42.29	0.18
−39.58	0.11
−39.99	0.15
−39.66	0.41
−40.61	0.12
−39.38	0.14
−39.60	0.53
−39.45	0.12
−36.46	0.33
−39.51	0.39

Table 7. Binding Energies and Diffusion Constants of the 14 Strongest-Bound Water Molecules at the {0$\bar{1}\bar{1}$} Surface

binding energy/ kJ mol^{-1}	diffusion constant/ 10^{-9} m^2 s^{-1}
−23.78	2.23
−26.82	1.68
−29.97	1.80
−30.06	0.50
−28.30	0.49
−29.77	2.24
−27.40	2.83
−28.05	1.16
−24.26	0.18
−25.24	0.68
−27.30	2.79
−29.79	2.69
−29.66	1.06
−29.21	1.94

and 144.65 mJ m^{-2} for {011}), the experimental value for γ_{Water} (72.88 mJ m^{-2}), and the estimate for $\gamma_{Resorcinol}$ for the polar *c*-axis (46.53 mJ m^{-2}) into the Dupre equation gives interfacial energies of −6.56 and −25.24 mJ m^{-2} for the {0$\bar{1}\bar{1}$} and {011} faces, respectively. These values are clearly very low and close to zero, the negative sign arising from the approximations involved. A low value is indeed expected for a polar substance such as resorcinol, which gives further confidence in both the force field being employed and the simulations.

Characterization of the Strongest Binding Sites. An attempt was made to determine the strongest binding sites on the two surfaces. The crystal−water binding energies of the 14 most strongly bound water molecules at each surface were determined and are tabulated in Tables 6 and 7, while the trajectory projections of these molecules are shown in Figure 6. These molecules and their coordinates were identified by calculating the binding energy of each water molecule in the surface layer with the crystal as a function of simulation time and then ranking the energies. From Tables 6 and 7, it is clear that the binding of the strongly bound water molecules is significantly and consistently stronger at the slower growing {011} face compared with that at the {0$\bar{1}\bar{1}$} face. The energy differences are reflected in the diffusion rate constants of the individual molecules, the diffusion constants being lower for the slower growing face. The trajectory projections in Figure 6 show that the binding sites on the slower growing face correspond to the isolated areas observed in the trajectory projections of the first water layer. These sites (being characterized by lower energy and lower diffusion) thus serve as strong binding sites for water, and the removal of this water could be the rate-limiting step in the growth of the {011} face. In contrast, the faster growing {0$\bar{1}\bar{1}$} face does not show any specific sites. The trajectory projections
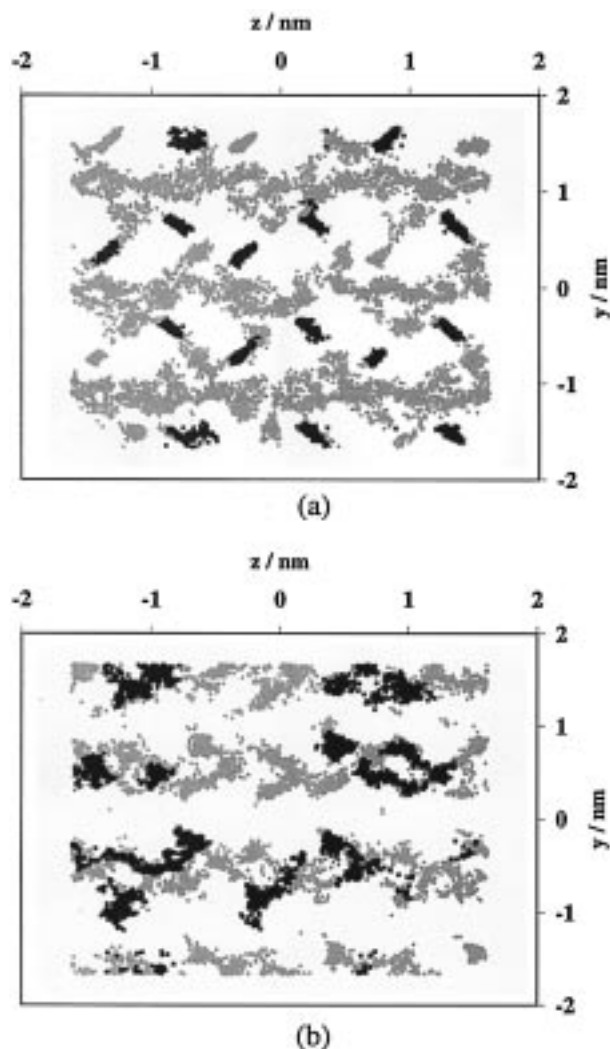
Figure 6. Center-of-mass trajectory projections for the strongest-bound water molecules (dark shading) superimposed on trajectory projections of all molecules in the first water layer (light shading), over a 20 ps period at the (a) {011} and (b) {0$\bar{1}\bar{1}$} surface.

of the strongly bound water molecules for this face do not appear to show these molecules being confined at any specific sites.

Snapshots of both the {011} and the {0$\bar{1}\bar{1}$} crystal surfaces showing the strongest-bound water molecules are given in Figures 7 and 8, respectively. The strong binding sites at the slow growing {011} surface are not (as expected) within the grooves running along the crystallographic a-axis (z direction of the simulation cell), but are located above the outermost part of the crystal surface. The water molecules at these sites all expose their oxygens toward the crystal surface but not their hydrogens. The molecules form strong hydrogen bonds with the limited number (one per two resorcinol molecules) of hydroxyl hydrogen atoms that are exposed at this surface. These water interactions are stronger than those with the aromatic hydrogens that are present both within the grooves and protruding from the surface. For the faster growing {0$\bar{1}\bar{1}$} surface, the strongest-bound water molecules generally orient with their hydrogen atoms pointing to the crystal surface. These are hydrogen-bonded to the exposed hydroxyl oxygen atoms of the resorcinol molecules. Some of the water molecules do not appear to be involved in hydrogen bonding. Furthermore, their location does not appear to be restricted to specific sites.

Simply focusing on the strongest binding sites may not be entirely useful in identifying a rate-limiting step for crystal

growth. A binding site at which the motion of a solvent is restricted, irrespective of the underlying mechanism, could be more important. For a solvent molecule trapped within a pocket, the binding may be weak, and yet its motion may be restricted due to a restriction in the degrees of freedom of the molecule imposed by the pocket. In view of this, the trajectory of the molecules in the surface layers was searched to identify molecules with the lowest diffusion constants. The slowest diffusing molecules were then ranked, and their locations were determined at various time intervals. The results complement the earlier analysis of the diffusion constants in segments of water along the x-axis. On the slower growing {011} face, the slowest diffusing molecules include not only the strongest-bound water molecules but also those within the channels on this face. The strongest-bound water molecules may play a role in restricting the motion of the molecules within the channels by influencing the water structure above the channels. On the faster growing {0$\bar{1}\bar{1}$} face, the picture is similar in that the slowest diffusing molecules include some of those within the shallow channels on this face as well as the strongest bound. An overall comparison between the two faces (as confirmed by Figure 5) indicates that water molecules at the slower growing face are more restricted in their motion than those at the faster growing face.

Discussion

The problem being addressed is how does the solvent, namely water, cause uneven relative growth of α-resorcinol crystals along the polar axis {011}. The key issue is the interaction of the solvent with the respective crystal faces and its effect on subsequent growth of the surfaces. Toward this end, molecular dynamics simulations of the crystal−water interface for both the {0$\bar{1}\bar{1}$} and the {011} interfaces have been carried out.

As to whether solvent binding retards or promotes crystal growth will, in principle, depend on whether the binding is confined to specific sites or is nonspecific, the strength of the binding, and the extent of supersaturation. Should the binding occur preferentially at specific sites, the role of the solvent will depend on whether the occupied sites correspond to the solute sites for the next growth layer. The various possibilities and expected outcomes are tabulated in Table 8.

When the solvent binding is nonspecific and weak, the solvent is expected to promote crystal growth. This is the solvent roughening theory, whereby the solvent molecules reduce the edge energy, thus lowering the two-dimensional nucleation barrier so as to enable the growth of the next layer to continue. In contrast, a stronger, nonspecific interaction between the solvent and the crystal surface is expected to retard the growth of the crystal surface.[5,6] In this case, desolvation is likely to be the rate-limiting step.

When solvent binding occurs at specific sites, there are at least two important situations that need to be considered. If the binding is at sites that correspond to the solute sites for the next growth layer, the solvent is expected to retard growth. Growth of the next solute layer cannot occur until the bound solvent molecules are displaced from the solute sites. The extent of inhibition of growth will depend on the strength of binding of the solvent molecules and on how the bound solvent molecules interact with the oncoming solute molecules. If the adsorbed solvent molecules neither block nor disrupt the interaction of the oncoming solute molecules, the effect of the solvent may be marginal and the solvent simply becomes occluded within the growing crystal.
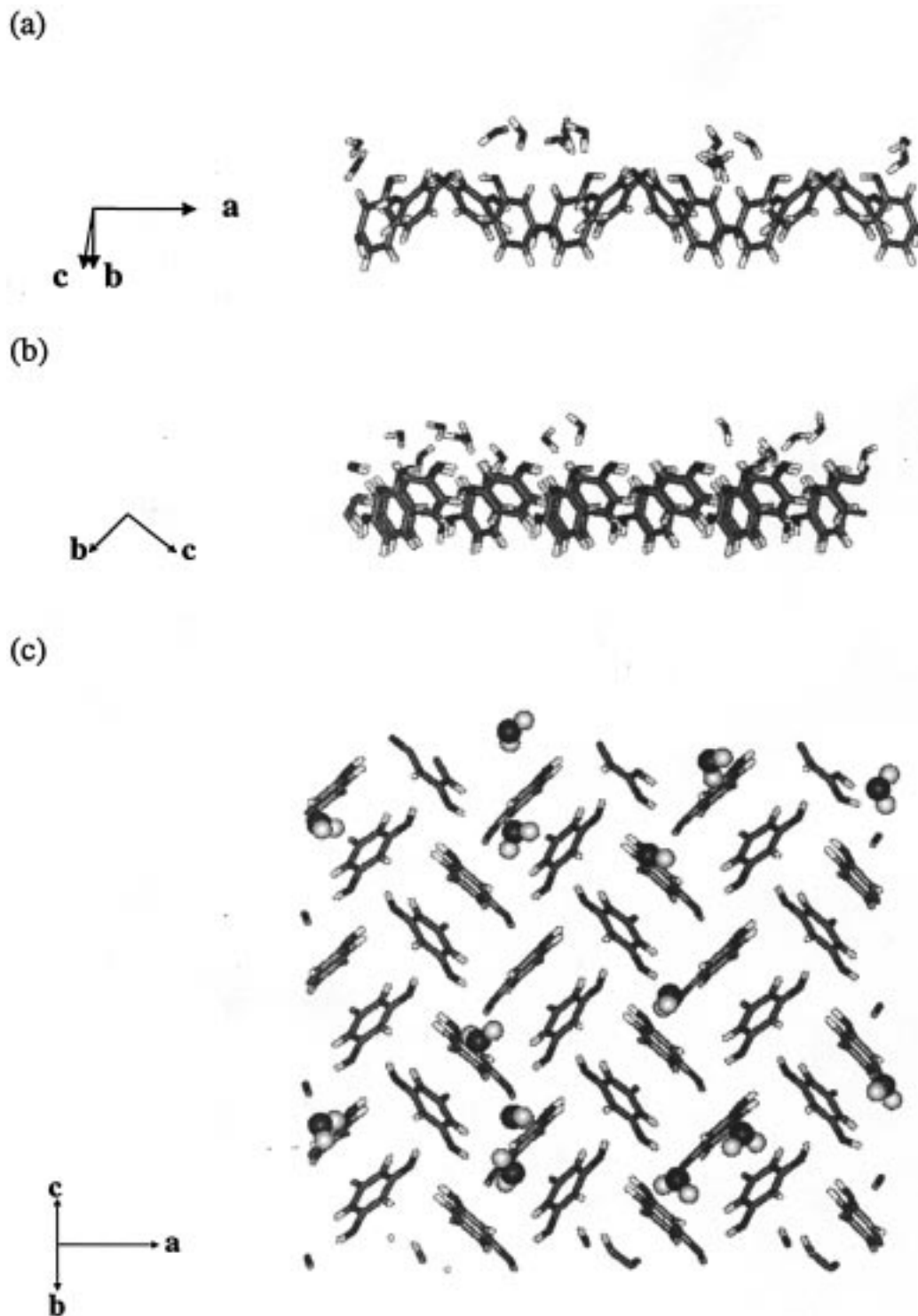
(a)

(b)

(c)
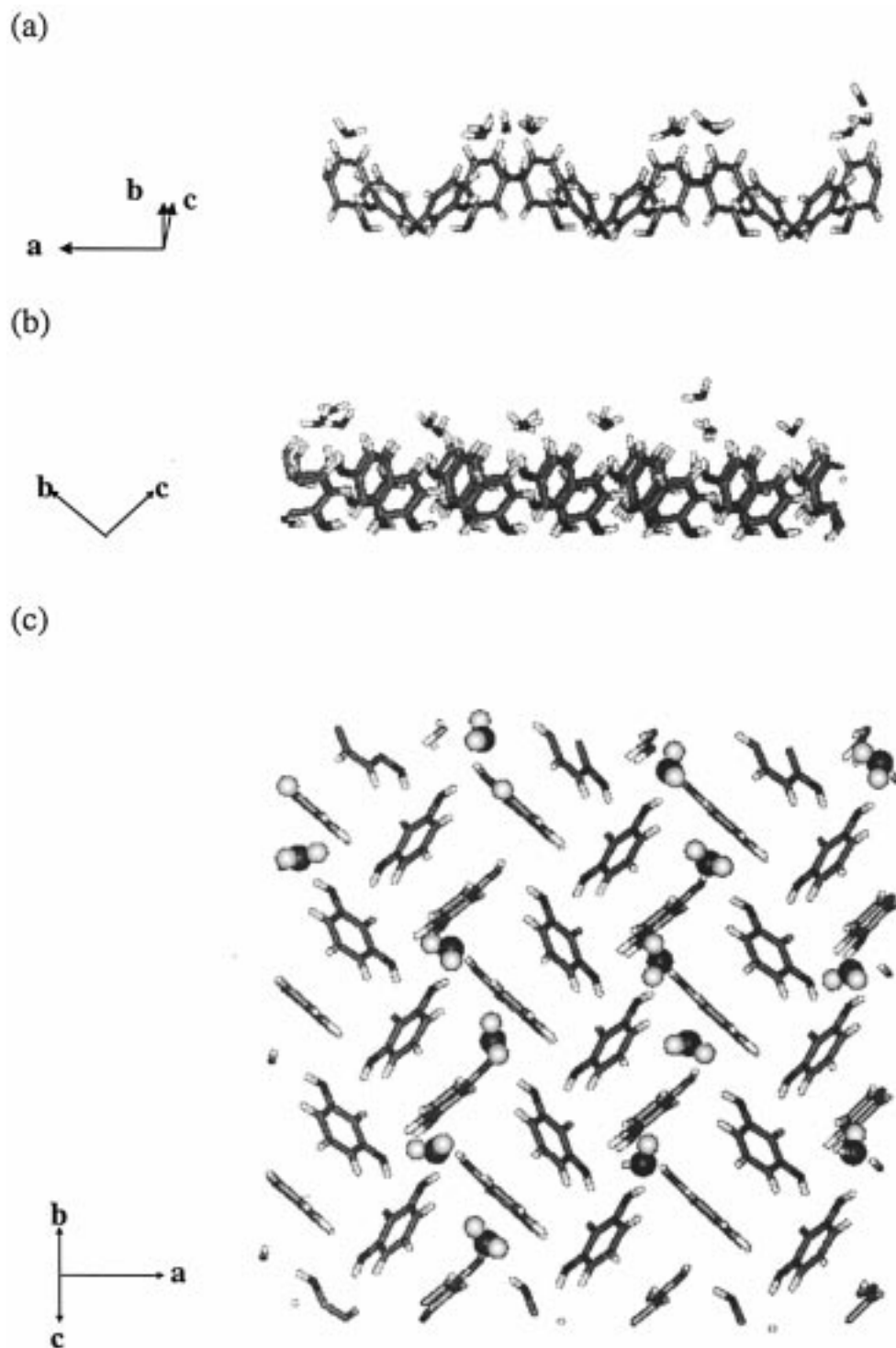
Figure 7. Snapshot of the slow growing {011} resorcinol crystal surface showing the strongest-bound water molecules, looking (a) along the $+b$ $-c$ direction, (b) along the a-axis, and (c) down on the crystal surface along the $+b$ $+c$ direction.

For solvent molecules binding at sites other than those corresponding to the solute sites of the next growth layer, there is a possibility that the solvent may promote growth. The actual effect of the solvent will depend on whether the solute sites are still accessible as well as on the strength of the binding. Inaccessible solute sites should lead to inhibition. Strong binding on nonsolute sites, while promoting the growth of the next layer, may inhibit the growth of the subsequent layer, as desolvation could then be the rate-limiting step. This would result in a cycle of slow−fast−slow−fast growth not too dissimilar to the relay mechanism proposed for the growth of (R,S)-alanine and α-glycine in water.[7]

For α-resorcinol the results from the MD simulations of the {011} and {01$\bar{1}$} crystal−water interfaces are consistent with stronger adsorption of water resulting in slower growth. At the slower growing {011} face, the average crystal−water binding energy is lower (that is, the binding of water is stronger) and the motion of the water molecules more restricted. Furthermore, this face is also characterized by strong, specific water-binding sites.

Examination of the water density close to the crystal surfaces does not shed any light as to whether there is any preferential affinity of the surfaces for water. Both surfaces appear to be strongly hydrophilic, being characterized by strong sharp peaks

(a)

(b)

(c)

Figure 8. Snapshot of the faster growing $\{0\bar{1}\bar{1}\}$ resorcinol crystal surface showing the water molecules with the lowest energy, looking (a) along the $+b\ -c$ direction, (b) along the a-axis, and (c) down on the crystal surface along the $-b$ and $-c$ direction.

Table 8. Possible Effects of Solvent Binding on Crystal Growth

type of binding	binding strength	expected outcome
nonspecific	weak	promotion
	strong	inhibition
specific: solute sites	weak	inhibition
	strong	inhibition
specific: nonsolute sites	weak	promotion
	strong	promotion−inhibition relay mechanism

close to the surface. The crystal−water interaction energies, however, are more discriminating. The energies indicate that

the water is more strongly adsorbed at the slower growing {011} face. The crystal−water interaction energy for this face is about 16% lower than the faster growing face (Table 5). The stronger interaction at this face is attributed to the extensive, strong C−H···O interactions with water and the larger accessible surface area due to the grooves.

One might assume that the effect of water could be attributed simply to the determined difference in the average crystal−water interaction energy. The average crystal−water interaction energy, however, may not be important, and the removal of one or more water molecules that are more strongly bound at

some specific sites could be the rate-limiting step in the crystal growth process. Thus, it is also necessary to characterize the strongest water-binding sites on the crystal surface. Such an analysis (Tables 6 and 7) indicates that there are indeed sites at which the water molecules are significantly more strongly bound and that they occur on the slower growing {011} face. The existence of these sites is also confirmed by the trajectory projections (Figure 6), which clearly reveal the islands of highly localized water molecules between the channels at the slower growing face. The binding sites, however, are not located within the grooves as one might expect. The sites are above the outermost part of the crystal surface, the interaction of the water here being with the limited number of hydroxyl hydrogen atoms that protrude from this surface. These interactions are stronger than those with the aromatic hydrogens within the grooves. The water diffusion data are entirely consistent with the picture emerging from the binding energy calculations. The effective diffusion of water at the surface of the slower growing {011} face is significantly lower compared with the respective value for the faster growing face (Table 4 and Figure 5). In general, for both crystal surfaces, the molecules occupying the channels have the lowest diffusion constant. For the slow growing {011} face, however, the strongest-bound water molecules that are located above the crystal surface also exhibit low diffusion rates (Table 7). This behavior is reflected in Figure 5, where the anisotropic diffusion constants show a small peak close to the surface of the slow growing face.

As to what exactly might be the rate-limiting step in the growth of the slower growing face is not clear. The strong binding sites, since they are located above the protrusions on the surface, might not be expected to interfere with solute attachment into the grooves. In which case, desolvation of the grooves would be the rate-limiting step. However, for the subsequent attachment of solute molecules, the removal of the water from the strong binding sites would be necessary, and this step would then be the rate-liming step. The strong binding sites may also have an indirect role in restricting the motion of the molecules within the grooves. This could be by way of dictating the water structure above the grooves.

That the water is retarding growth at the {011} face is consistent with conclusions of previous studies that have attempted to address this question.[6,16,29] The crystal−water interaction energies compare well with those obtained by Khoskhoo and Anwar:[6] −134 mJ m^{-2} ({011} face) and −130 mJ m^{-2} ({0$\bar{1}\bar{1}$} face) compared with −145 and −126 mJ m^{-2}, respectively, for the present study. These differences in energy can be attributed to the fact that the current simulations employ a larger system, better force field parameters, and sample phase space more thoroughly. In the experimental study of Davey et al.[29] the kinetics of the crystal faces {011} and {0$\bar{1}\bar{1}$} of

α-resorcinol were measured as a function of supersaturation. The rate of growth of the {011} face was, at all supersaturations, lower than that of the {0$\bar{1}\bar{1}$} face and exhibited a dead zone at low supersaturations. In contrast, the {0$\bar{1}\bar{1}$} face did not show any detectable dead zone and growth appeared to occur even at very low supersaturations. This dead zone behavior is similar to that observed for crystal growth in the presence of additives that inhibit growth. It was, therefore, concluded that the dead zone and the lower growth rate at the {011} face resulted from strong adsorption of water at this face.

The present simulations provide categorical evidence for the association of strong, selective binding and restricted motion of water with slower crystal growth for α-resorcinol. The full mechanism of action of the solvent, however, still remains elusive. We do not yet have a dynamic picture of the molecular processes that occur as solute competes for sites on the growing crystal surface in the presence of the solvent. Long time-scale simulations of the crystal interface with a supersaturated solution could significantly enhance our understanding.

Finally, we would like to make a technical comment regarding the simulation methodology. Calculation of the Coulombic interactions using Ewald summation is rigorous but can significantly increase the computing requirement, the effect of which is to limit the time scales of the simulations. Crystal growth processes are relatively slow, and much insight could be gained from exploring longer time scales in the simulations. It is therefore important to ascertain whether Ewald summation is necessary for simulations of crystal−solvent interfaces for polar, molecular systems. For metal−water surfaces, Ewald summation has been considered to be essential.[27] Comparison of the two simulations conducted in the present study, that is, with and without Ewald, shows that the features of the simulations and the properties calculated are essentially identical. The crystal−water interaction energies were −145 mJ m^{-2} ({011} face) and −126 mJ m^{-2} ({0$\bar{1}\bar{1}$} face) for the Ewald simulation and −150 mJ m^{-2} ({011} face) and −126 mJ m^{-2} ({0$\bar{1}\bar{1}$} face) for the non-Ewald simulation. The density profiles (not shown) and the diffusion constants are also very similar. In view of this, it seems reasonable to carry out simulations of the crystal−solvent interfaces for polar, molecular crystals without employing Ewald summation. A qualification is that the cutoff is similar or larger than that employed in the present simulations (1.1 nm).

In summary, molecular dynamics simulations of the {011} and {0$\bar{1}\bar{1}$} resorcinol−water interfaces have been carried out. The simulations reveal that the water molecules are more strongly and selectively adsorbed at the slower growing {011} face and that their motion is more localized. The inference is that the stronger binding and restricted motion of the water molecules at the {011} surface serve to retard crystal growth at this surface.

(29) Davey, R. J.; Milisavljevic, B.; Bourne, J. R. *J. Phys. Chem.* **1988**, *92*, 2032−2036.

(30) Robertson, J. M. *Proc. R. Soc. London* **1936**, 79−99.